

## HADRONIC RESONANCES IN LATTICE QCD\*

S. PRELOVSEK<sup>a,b,†</sup>, C.B. LANG<sup>c</sup>, L. LESKOVEC<sup>b</sup>, D. MOHLER<sup>d</sup>  
R.M. WOLOSHYN<sup>e</sup>

<sup>a</sup>Physics Department, University of Ljubljana, 1000 Ljubljana, Slovenia

<sup>b</sup>Jozef Stefan Institute, 1000 Ljubljana, Slovenia

<sup>c</sup>Institut für Physik, Universität Graz, 8010 Graz, Austria

<sup>d</sup>Fermilab, Batavia, 60510-5011, Illinois, USA

<sup>e</sup>TRIUMF, 4004 Wesbrook Mall, Vancouver, BC V6T 2A3, Canada

(Received June 24, 2013)

We discuss how masses and widths of hadron resonances are extracted from lattice QCD. Recent lattice results on the light, strange and charm meson resonances are reviewed. Their properties are revealed by simulating the corresponding scattering channels  $\pi\pi$ ,  $K\pi$  and  $D\pi$  on the lattice and extracting the scattering phase shifts. In particular, we address the resonances  $\rho$ ,  $D_0^*(2400)$ ,  $D_1(2430)$ ,  $K^*$ ,  $\kappa$  and  $K_0^*(1430)$ .

DOI:10.5506/APhysPolBSupp.6.879

PACS numbers: 11.15.Ha, 12.38.Gc, 14.40.Df, 14.40.Lb

## 1. Introduction

Most hadrons are resonances, *i.e.*, they decay extremely fast via the strong interaction. Yet most of these resonances were studied in lattice QCD assuming the so-called narrow width approximation, that is ignoring their strong decay. Up to now, only the  $\rho$  meson has been simulated properly as a resonance by several groups and its width was extracted (see [1–3] and references therein). Recently, the first simulation of charmed resonances in  $D\pi$  scattering was performed [4], while the strange scalar and vector resonances were addressed by simulating  $K\pi$  scattering [5]. This paper briefly reviews the main results and methods that were employed. Recent lattice results of resonances are reviewed in [6].

---

\* Presented at the Workshop “Excited QCD 2013”, Bjelašnica Mountain, Sarajevo, Bosnia–Herzegovina, February 3–9, 2013.

† [sasa.prelovsek@ijs.si](mailto:sasa.prelovsek@ijs.si)

## 2. Meson–meson scattering in a resonant channel on the lattice

Meson resonances are formed in the strong scattering  $M_1 M_2 \rightarrow R \rightarrow M_1 M_2$  in partial wave  $l$ . They exhibit a Breit–Wigner-like resonance behavior of  $\delta$ , amplitude  $T$  and  $\sigma(s) \propto \sin^2 \delta(s)$

$$T = \frac{-\sqrt{s} \Gamma(s)}{s - m_R^2 + i\sqrt{s} \Gamma(s)} = e^{i\delta(s)} \sin \delta(s), \quad \Gamma(s) = \frac{(p^*)^{2l+1}}{s} g^2, \quad (1)$$

$$\frac{(p^*)^{2l+1} \cot \delta}{\sqrt{s}} = \frac{1}{g^2} (s - m_R^2), \quad (2)$$

where  $\Gamma(s)$  is parametrized in terms of the phase space and the  $R \rightarrow M_1 M_2$  coupling  $g$ . The combination  $(p^*)^{2l+1} \cot \delta / \sqrt{s}$  is linear in  $s$  for a single Breit–Wigner resonance, which allows the extraction of  $m_R$  and  $g$  (and, therefore, the width) using a linear fit (2) once the phase shifts  $\delta(s)$  are determined from the lattice. So, the goal is to simulate the scattering on the lattice and determine the scattering phase shift  $\delta(s)$ .

For this purpose, one computes the correlator  $C_{ij}(t) = \langle 0 | \mathcal{O}_i(t) \mathcal{O}_j(0) | 0 \rangle$ . We use the interpolators  $\mathcal{O} = M_1(\vec{p}_1) M_2(\vec{p}_2) = \bar{q}_1 \Gamma_1 q'_1 \bar{q}_2 \Gamma_2 q'_2$  that create two-meson states with definite momenta, and  $\mathcal{O} = \bar{q} \Gamma q'$  that couple well to the resonances. Both are constructed to have the quantum numbers<sup>1</sup> of the desired channel and total momentum  $\vec{P} = \vec{p}_1 + \vec{p}_2$ . The interpolators  $\mathcal{O}$  couple, in general, to all physical eigenstates  $n$  and each of them evolves as  $e^{-E_n t}$  in the Euclidean time, so  $C_{ij}(t) = \sum_n A_{ij}^{(n)} e^{-E_n t}$ .

We calculate the correlators  $C_{ij}(t)$  using a powerful distillation method [7], which enables the calculation of all the necessary Wick contractions. Our study is based on 280 gauge configurations with  $a \simeq 0.124$  fm and dynamical Wilson–Clover  $u/d$  quarks corresponding to  $m_\pi \simeq 266$  MeV. A rather small volume  $16^3 \times 32$  makes the distillation method [7] feasible. The valence charm quark is treated using the Fermilab method described in [4]. The resulting  $C_{ij}(t)$  allows the extraction of the few lowest eigen energies  $E_n$  via the generalized eigenvalue method.

## 3. Physics information based on the energy spectrum $E_n(L)$

The scattering energy levels (black circles and gray (green) circles in Fig. 1) appear at  $E(L) = \sqrt{m_1^2 + \vec{p}_1^2} + \sqrt{m_2^2 + \vec{p}_2^2} + \Delta E(L)$  with discrete  $\vec{p}_i = \vec{n} \frac{2\pi}{L}$  due to the periodic boundary conditions in space. The energy shift  $\Delta E(L)$  in the finite volume is due to the strong interaction of the two

<sup>1</sup> On a finite discrete lattice, the interpolators  $\mathcal{O}$  have to transform according to irreducible representations of the symmetry group related to the center-of-momentum frame.

mesons. The negative shift of the lowest level for  $I = 1/2$  s-wave scattering of  $K\pi$ ,  $D\pi$  and  $D^*\pi$  in Fig. 1 indicates attractive interaction. The positive shift for  $K\pi$  with  $I = 3/2$  indicates repulsive interaction. In addition to the scattering levels near the dashed lines, the presence of resonances in  $I = 1/2$  channels leads to extra levels (stars and crosses for  $K\pi$ ; squares and diamonds for  $D\pi$ ). These indicate s-wave resonances  $D_0(2400)$  in  $D\pi$ ,  $D_1(2420)$  and  $D_1(2430)$  in  $D^*\pi$ ,  $K_0(1430)$  in  $K\pi$ , as well as p-wave resonances  $K^*(892)$ ,  $K^*(1410)$ ,  $K^*(1680)$  in  $K\pi$  [4, 5]. We do not find an additional level due to  $\kappa$  [5], which is in agreement with the fact that the experimental phase shift does not reach  $90^\circ$  below 1 GeV. We also do not find additional energy levels in  $I = 3/2$  channels, in line with absence of the exotic resonances in experiment.

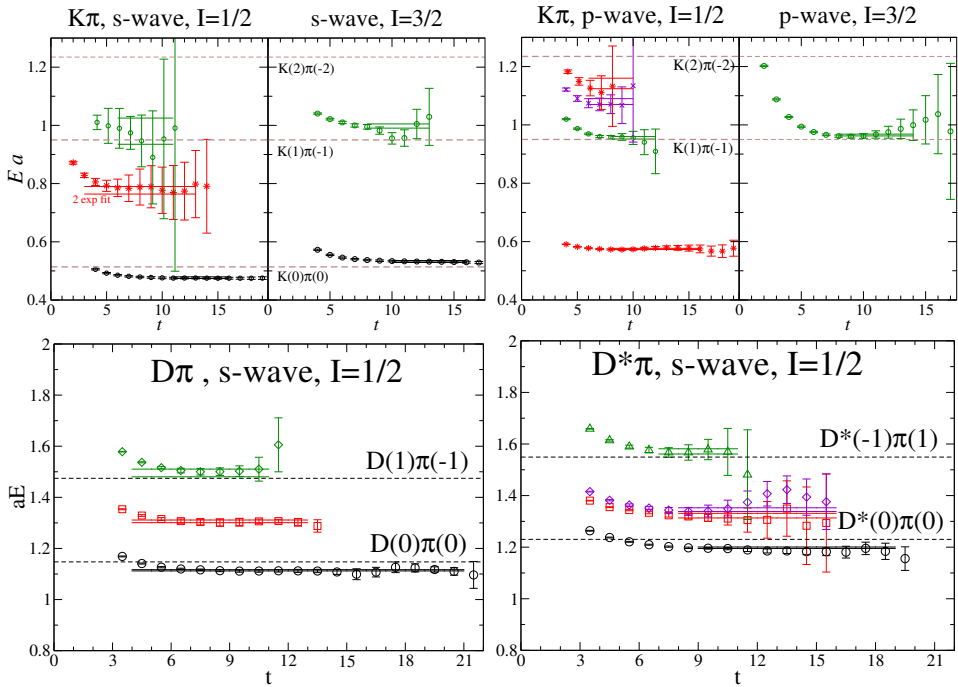


Fig. 1. The energy levels (effective masses of eigenvalues) for  $K\pi$  ( $J^P = 0^+, 1^-$ ),  $D\pi$  ( $J^P = 0^+$ ) and  $D^*\pi$  ( $J^P = 1^+$ ) scattering with  $\vec{P} = 0$  [4, 5]. Dashed lines indicate energies of non-interacting scattering states.

#### 4. Phase shifts and resonance parameters

The energy shift in finite volume reveals the attractive or repulsive nature of the interaction. However, it also rigorously renders the phase shift for the elastic scattering in the infinite volume via the Lüscher's relation. In

particular, the energy level  $E(L)$  for a scattering system with momenta  $\vec{P}$  renders the elastic phase shift  $\delta(s)$  at  $s = E^2 - \vec{P}^2$  in partial wave  $l$ . Note that the extraction of  $\delta(s)$  is straightforward only when the partial-wave mixing due to the discrete symmetry is absent or negligible, which usually holds well for  $\vec{P} = 0$ , but holds rarely for the scattering of two particles with different mass and  $\vec{P} \neq 0$  [8].

The  $\pi\pi \rightarrow \rho \rightarrow \pi\pi$  was simulated for three different  $\vec{P}$  in [1] and five energy levels lead to resonant phase shift in Fig. 2. The linear fit of the resulting  $p^{*3} \cot \delta / \sqrt{s}$  (2) leads to  $g_{\rho\pi\pi}^{\text{lat}} \equiv \sqrt{6\pi}g = 5.13 \pm 0.20$  and  $m_\rho^{\text{lat}} = 792 \pm 10$  MeV compared to  $g_{\rho\pi\pi}^{\text{exp}} = 5.97$  and  $m_\rho^{\text{exp}} = 775$  MeV. This is the only resonance where proper lattice treatment has reached a certain level of maturity (see [1–3] and references therein). A particularly detailed and impressive shape of the resonant phase shift curve was achieved in [3] at a heavier pion mass  $m_\pi \simeq 400$  MeV.

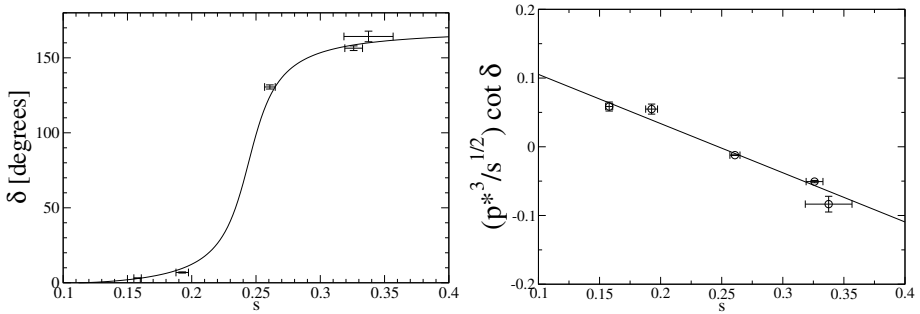


Fig. 2. Left: the p-wave  $\pi\pi \rightarrow \pi\pi$  phase shift  $\delta$  with  $I = 1$  [1]. Right: the corresponding  $(p^*)^3 \cot \delta / \sqrt{s}$  (2).

Over the past year, we performed the first simulation of the  $K\pi$  [5],  $D\pi$ ,  $D^*\pi$  [4] and  $\rho\pi$  [9] scattering and the corresponding resonances. Since this involves scattering of two particles with different masses, we considered only  $\vec{P} = 0$  when the mixing of different  $l$  is absent or negligible [8].

The energy levels for  $K\pi$  scattering in Fig. 1 lead to the phase shifts in Fig. 3 for s-wave and p-wave with  $I = 1/2, 3/2$ . These are in qualitative agreement with the experimental ones.

Next, we concentrate on the charmed resonances that appear in  $D\pi$  and  $D^*\pi$ . The three energy levels for  $D\pi$  s-wave scattering in Fig. 1 lead to the phase shifts [4], and the linear fit (2) over three points leads to  $m$  and  $\Gamma$  (or  $g$ ) for the broad  $D_0^*(2400)$  in Table I. The analysis of  $D^*\pi$  spectrum with  $J^P = 1^+$  is more complicated since there are two nearby resonances in experiment, as evidenced by two nearby levels indicated by diamonds and squares. We find that the level represented by squares is due to the

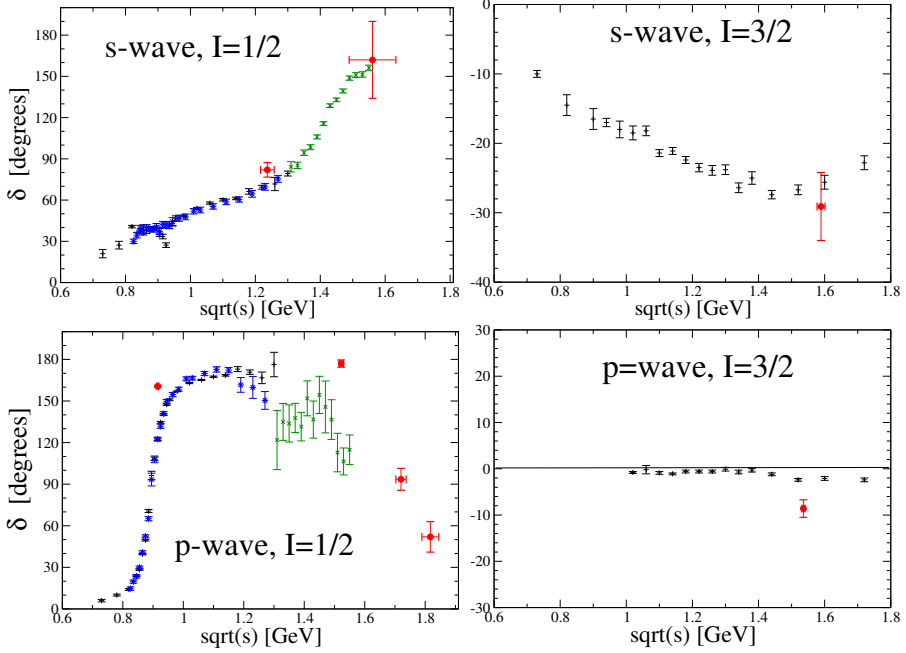


Fig. 3. The  $K\pi$  phase shifts  $\delta_\ell^I$  in channels  $l = 0, 1$  and  $I = 1/2, 3/2$  as a function of  $K\pi$  invariant mass  $\sqrt{s}$ . The lattice results are given by the grey/red circles (they apply for  $m_\pi \simeq 266$  MeV) [5], while the other points are experimental phase shifts.

narrow  $D_1(2420)$  which decays only in d-wave in the  $m_c \rightarrow \infty$  limit. In this limit, the remaining three levels are related to s-wave  $D^*\pi$  scattering which is dominated by the broad  $D_1(2430)$ . A linear fit (2) through these three points leads to the mass and the width for the broad  $D_1(2430)$  in Table I.

TABLE I

The charmed resonance masses (with respect to  $\bar{m} \equiv \frac{m_D + 3m_{D^*}}{4}$ ) and the couplings  $g$ , which parametrize the widths  $\Gamma = g^2 p^*/s$ . The experimental couplings  $g$  are derived from total widths.

	$m_{D_0^*(2400)} - \bar{m}$	$g_{D_0^*(2400) \rightarrow D\pi}$	$m_{D_1(2430)} - \bar{m}$	$g_{D_1(2430) \rightarrow D\pi}$
Lat. [4]	$351 \pm 21$ MeV	$2.55 \pm 0.21$ GeV	$381 \pm 20$ MeV	$2.01 \pm 0.15$ GeV
Exp.	$347 \pm 29$ MeV	$1.92 \pm 0.14$ GeV	$456 \pm 40$ MeV	$2.50 \pm 0.40$ GeV

The resulting masses and widths of  $D_0^*(2400)$  and  $D_1(2430)$  agree quite well with the experimental ones. Since  $D_0^*(2400)$ , located at  $\simeq 2318$  MeV, is very close to its strange partner  $D_{s0}^*(2317)$ , several authors proposed

that  $D_0^*(2400)$  has a sizable tetraquark component  $\bar{c}\bar{s}su$ . We get  $m_{D_0^*(2400)}$  near the experimental value without explicitly incorporating the additional strange valence pair<sup>2</sup>.

The compilation of the  $D$  meson spectrum in Fig. 4 shows quite good agreement with experiment [4]. The masses of broad resonances  $D_0^*(2400)$  and  $D_1(2430)$  are extracted as explained above. Other four low-lying  $J^P = 0^-, 1^-, 1^+, 2^+$  states are stable or very narrow, so they were simulated using  $\mathcal{O} = \bar{c}\Gamma u$  and  $m = E$  ( $\vec{P} = 0$ ) is employed like in all previous simulations. This narrow-width approximation is applied also for the excited states in  $J^P = 0^-, 1^-, 2^-$  channels, which are compared to the states observed by the BaBar in 2010 [10]; unfortunately, these are not yet confirmed by any other experiment.

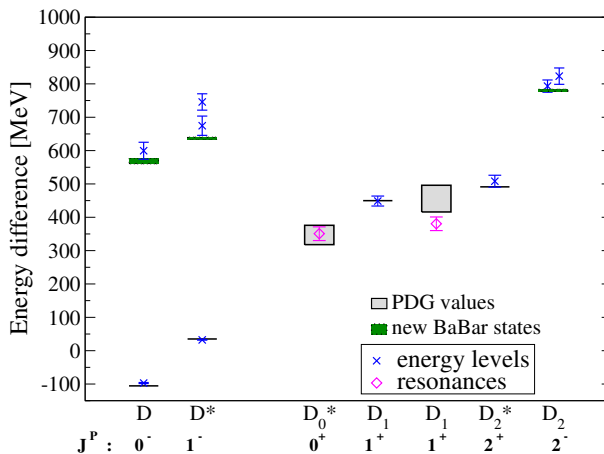


Fig. 4. Energy differences  $m - \frac{1}{4}(m_D + 3m_{D^*})$  for  $D$  mesons on lattice [4] and in experiment; the reference mass is  $\bar{m} = \frac{1}{4}(m_D + 3m_{D^*}) \approx 1971$  MeV in experiment. Diamonds (magenta) give masses for states simulated as resonances [4]. Masses extracted as energy levels on a finite lattice are displayed as crosses (blue) [4].

The scattering lengths for  $K\pi$ ,  $D\pi$  and  $D^*\pi$  were also extracted in [4, 5].

In conclusion,  $\rho$  is the only resonance that was treated properly by several lattice groups up to now. We presented the first results of the strange and charmed resonances based on the simulation of the corresponding scattering channels.

We thank Anna Hasenfratz for providing the gauge configurations. Fermilab is operated by Fermi Research Alliance, LLC under Contract No. De-AC02-07CH11359 with the United States Department of Energy.

<sup>2</sup> The  $\bar{s}s$  cannot appear as intermediate state in our simulation without dynamical  $s$ .

## REFERENCES

- [1] C.B. Lang, D. Mohler, S. Prelovsek, M. Vidmar, *Phys. Rev.* **D84**, 054503 (2011).
- [2] C. Pelissier, A. Alexandru, *Phys. Rev.* **D87**, 014503 (2013).
- [3] J.J. Dudek, R.G. Edwards, C.E. Thomas, *Phys. Rev.* **D87**, 034505 (2013).
- [4] D. Mohler, S. Prelovsek, R.M. Woloshyn, *Phys. Rev.* **D87**, 034501 (2013).
- [5] C.B. Lang, L. Leskovec, D. Mohler, S. Prelovsek, *Phys. Rev.* **D86**, 054508 (2012).
- [6] D. Mohler, *PoS LATTICE2012*, 003 (2012) [[arXiv:1211.6163](#) [[hep-lat](#)]].
- [7] M. Peardon *et al.*, *Phys. Rev.* **D80**, 054506 (2009).
- [8] L. Leskovec, S. Prelovsek, *Phys. Rev.* **D85**, 114507 (2012).
- [9] S. Prelovsek, C.B. Lang, D. Mohler, M. Vidmar, *PoS LATTICE2011*, 137 (2011) [[arXiv:1111.0409](#) [[hep-lat](#)]].
- [10] P. del Amo Sanchez *et al.* [BaBar Collaboration], *Phys. Rev.* **D82**, 111101 (2010).